ANNALS OF GEOPHYSICS, 69, 1, S112, 2026; doi:10.4401/ag-9319
OPEN ACCESS

Integrating the FXLand network into the real-time earthquake surveillance and monitoring system of Italy

Marina Pastori[*,1], Diana Latorre[1], Milena Moretti[1], Lucia Margheriti[1], Davide Piccinini[2], Salvatore Claudio Alparone[4], Ornella Cocina[4], Antonio Costanzo[1], Marc-Andre Gutscher[3], Mario La Rocca[5], Alessandro Marchetti[1], Shane Murphy[3], Anna Nardi[1], Chastity Aiken[3] and Focus Working Group (2021)[6]

(1) Istituto Nazionale di Geofisica e Vulcanologia, Osservatorio Nazionale Terremoti, Italy
(2) Istituto Nazionale di Geofisica e Vulcanologia, Sezione di Pisa, Italy
(3) Geo-Ocean UMR6538, CNRS, Ifremer, Université Bretagne Occidentale, Université Bretagne Sud, France
(4) Istituto Nazionale di Geofisica e Vulcanologia, Osservatorio Etneo, Italy
(5) Università della Calabria, Laboratorio di Sismologia, Italy
(6) https://progetti.ingv.it/it/focus#focus-working-group

Article history: received February 28, 2025; accepted January 26, 2026

Abstract

The Ionian margin of southern Italy is one of the most complex geodynamic regions in the central Mediterranean, where ongoing convergence between the African and Eurasian plates results in intense seismic activity and highly heterogeneous crustal structures. To improve seismic monitoring in this region, within the framework of the ERC Advanced Grant FOCUS (2018-2025), a temporary onshore seismic network (FXLand) was deployed along the Ionian coasts of Sicily and Calabria from December 2021 to June 2023, complementing a marine array of ocean-bottom seismometers operating during the same period.

In this study we describe the deployment and performance of the 13 temporary broadband stations of FXLand. The network was integrated in real time into the Italian national seismic surveillance system, enhancing data availability and coastal network geometry. During the deployment, FXLand recorded, more than 1,500 local earthquakes and more than 200 teleseismic events with magnitude $M \geq 6$.

We also present results from the analysis of three seismic sequences that occurred during the network operational period. The application of a Template Matching technique to the combined permanent station and FXLand network dataset, we significantly increased the number of detected low-magnitude earthquakes in onshore area, improving catalog completeness compared to real-time surveillance and Italian Seismic Bulletin. On the other hand, the offshore sequence highlights the main limitations of land-based networks in detecting and accurately locating submarine seismicity. The integration of marine observations from the ocean-bottom seismometer network in the Ionian Sea is expected to provide substantial improvements in the detection and location accuracy of offshore earthquakes, contributing to a more complete characterization of seismic activity along the Ionian margin.

Keywords: Focus Project; Fxland Temporary Network; Seismic Surveillance; Real-Time Monitoring; Bollettino Sismico Italiano

1. Introduction

1.1 Seismotectonic framework

The Ionian margin of southern Italy represents one of the most complex and seismically active regions of the central Mediterranean. The area hosts the Calabrian Arc subduction system, where the African plate is converging beneath Eurasia at a rate of ~3-5 mm/yr, yellow arrows in Fig. 1 (Serpelloni et al., 2007; 2010; D'Agostino et al., 2008; Devoti et al., 2008). This geodynamic configuration has produced the Calabrian accretionary prism, a large wedge of deformed Plio-Quaternary sediments bounded to the southwest by the Malta Escarpment and to the northeast by the Apulian Platform (Rossi and Sartori, 1981; Fiorentino et al., 2025). A prominent NW-SE high-deformation crustal zone connects the prism's frontal thrust to the eastern coast of Sicily and intersects several major crustal structures, including the north part of the Alfeo-Etna Fault System, a key right-lateral strike-slip system linking offshore deformation to the southeastern flank of Mt. Etna (Fig. 1) (Polonia et al., 2011; Gutscher et al., 2017; Maesano et al., 2020).

Recent seismological and geophysical studies further clarify how deformation along the eastern Sicilian margin is partitioned between onshore and offshore structures. High-resolution seismic imaging and focal-mechanism analyses highlight the kinematic continuity between the Timpe fault system on Mt. Etna's southeastern flank

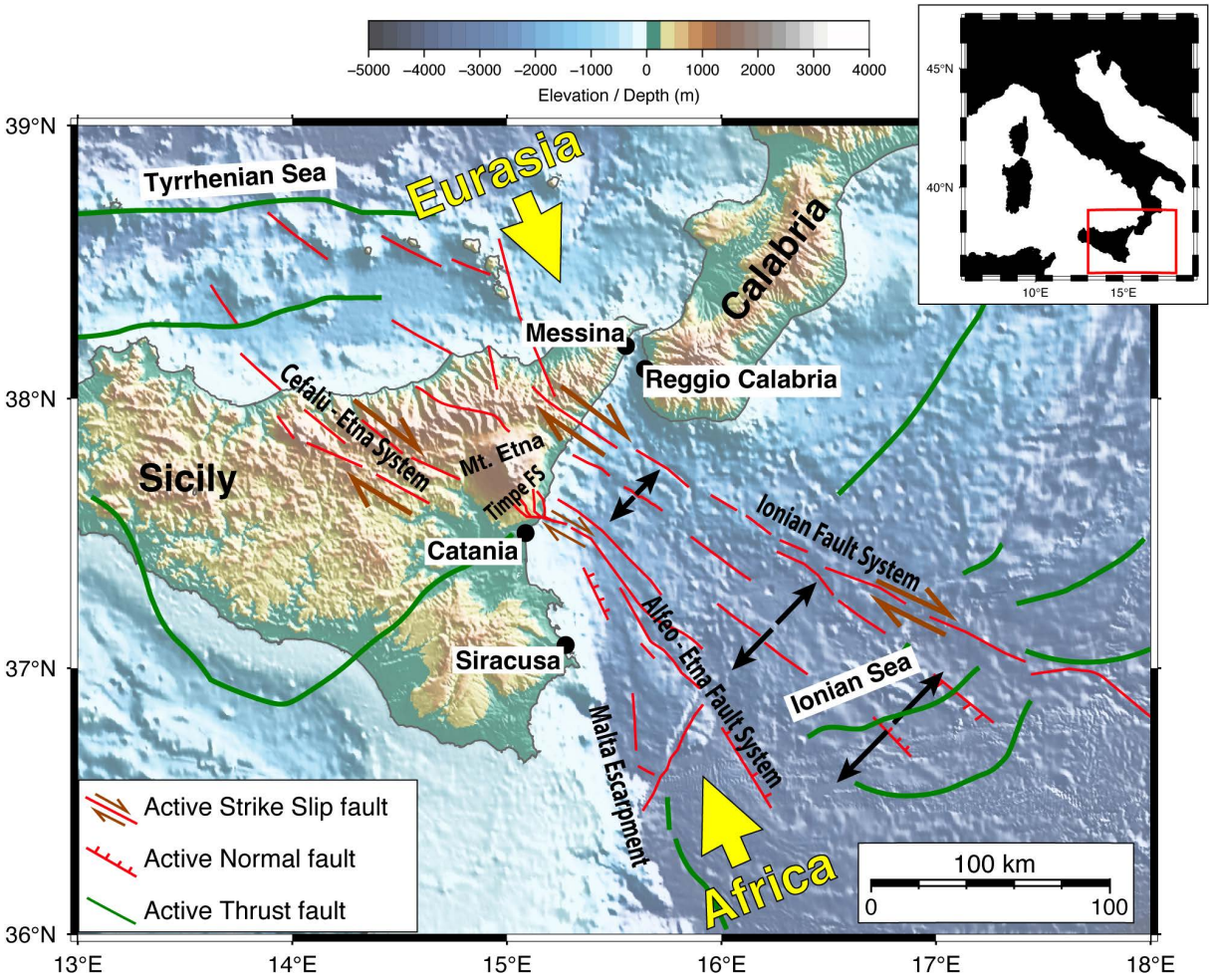

Figure 1. Simplified tectonic framework of eastern Sicily and southern Calabria-Ionian Sea region (modified after Sgroi et al., 2025, and Polonia et al., 2016). The map shows topography and bathymetry (color scale in meters) alongside the main active tectonic structures. Yellow arrows indicate the relative convergence between the African and Eurasian plates, while black arrows show extensional deformation within the western lobe of the Calabrian Arc accretionary wedge. Major tectonic elements include, among others, the Alfeo-Etna Fault System, the Ionian Fault System, and the Malta Escarpment

and the offshore Alfeo-Etna Fault System, a major dextral transtensional shear zone extending into the western Ionian Sea (Polonia et al., 2016; Gambino et al., 2022). Earthquake hypocenters recorded in this sector delineate a shallow, highly active crustal volume, where strike-slip and oblique-normal mechanisms align with the mapped fault traces, indicating that right-lateral shear is locally accommodated through releasing bends and short extensional segments. This integrated onshore-offshore deformation pattern provides a structural framework that explains both the clustering of earthquakes on Etna's submarine eastern flank and the transtensional morphologies observed along the upper slope of the Ionian margin, reinforcing the interpretation of the Alfeo-Etna Faultsystem as a key element of the evolving plate boundary in this sector.

In this region, active deformation is accommodated by a combination of subduction-related thrusting, strike-slip faulting, and transtensional processes, resulting in a heterogeneous stress field and widespread seismicity (Sgroi et al., 2021; 2025). Offshore geophysical surveys have identified multiple fault systems, such as the Alfeo-Etna Fault System, that likely contribute to strain partitioning along the margin (Maesano et al., 2020; Gambino et al., 2022). Recent structural and seismotectonic analyses in southern Calabria (Giuffrida et al., 2023; Maesano et al., 2018) further highlight the complexity of crustal deformation and the potential interaction between onshore and offshore fault systems. Generally, seismicity is distributed over a wide area but clusters mainly (i) along the Hyblean Plateau near the Malta Escarpment, (ii) on the submarine eastern flank of Mt. Etna, (iii) offshore Taormina, and (iv) in the southern Calabrian offshore, where focal mechanisms indicate the coexistence of extensional and strike-slip regimes (Sgroi et al., 2021).

Historically, eastern Sicily and Calabria have experienced several devastating earthquakes and tsunamis, including the 1169, 1693, 1783, and 1908 events, as documented in the Catalogue of Strong Earthquakes in Italy (CFTI5Med; Guidoboni et al., 2018; 2019) However, the exact seismogenic sources of many of these earthquakes remain debated, largely due to the lack of permanent offshore instrumentation and the limited resolution of marine geophysical datasets. The database of individual seismogenic sources (DISS Working group, 2025; Basili et al., 2008) identifies numerous potential crustal and subduction-related sources along the Ionian margin, many of which are classified as poorly constrained or debated, particularly offshore. These uncertainties highlight the need for dense, high-quality seismic observations to better characterize active structures and reduce epistemic uncertainty in regional hazard models.

The official Italian Seismic Hazard Model (MPS04-S1, http://esse1-gis.mi.ingv.it/; Stucchi et al., 2011; Meletti et al., 2006) identifies the Ionian sector of eastern Sicily and southern Calabria as one of the regions with the highest expected ground motions in Italy, with PGA values exceeding ~0.25 g (10% probability of exceedance in 50 years). This elevated hazard reflects the coexistence of subduction, crustal faulting, and volcanic processes, making the area a priority target for enhanced seismic monitoring.

1.2 The FOCUS project and the FXLand seismic network

Given the uncertainties surrounding the offshore fault systems and the need to improve earthquake detection capability along the Ionian margin, the *Fiber Optic Cable Use for Seafloor Studies of Earthquake* (FOCUS) project was funded within the ERC Horizon framework from October 2018 to September 2025. FOCUS seeks to demonstrate the potential of Distributed Acoustic Sensing (DAS) and fiber-optic reflectometry for detecting small seafloor deformation across active submarine faults. The eastern Sicilian margin is an ideal test site, as the EMSO Catania seafloor cable intersects the north part of the Alfeo-Etna Fault System only ~20 km offshore, providing a unique opportunity to monitor an active fault system in real time (Gutscher et al., 2017).

FOCUS experiment was designed to strengthen the regional monitoring infrastructure by integrating temporary networks both offshore and onshore. The offshore component, FXOBS (FDSN code XH; https://www.fdsn.org/networks/detail/XH_2022/ last accessed February 2025), consists 29 ocean-bottom seismometers deployed between 16 January 2022 and 26 February 2023 at water depths reaching ~3000 m. Twenty OBSs (SG and BB stations) were deployed during the FOCUS X2 cruise in January 2022, while an additional nine LT stations were deployed in August 2022 aboard the R/V Tethys II. All instruments were successfully recovered in February 2023; however, 5 BB and 6 LT OBSs were redeployed to optimize coverage of the Alfeo fault system until August 2023. The coordinates of the OBS installations for the two deployment phases are provided in Tables S1 and S2 in the Supplementary Material. The onshore component, FXLand (FDSN code 1J; https://www.fdsn.org/networks/detail/1J_2021/ last accessed February 2025), consists of 13 broadband seismic stations installed along the Ionian coasts of Sicily and Calabria.

The deployment was carried out by INGV's Osservatorio Nazionale Terremoti (ONT) and Osservatorio Etneo (OE), in collaboration with the University of Calabria (UniCal). FXLand operated between December 2021 and June 2023 and was fully integrated into the INGV real-time surveillance system, contributing to the routine detection and manual revision of seismicity reported in the Italian Seismic Bulletin (BSI). During its operational period, the network recorded more than 1,500 local and 200 teleseismic (Mw ≥6) earthquakes. The overall configuration of the offshore and onshore networks, together with the seismicity considered in this study, is shown in Fig. 2.

FXLand partly overlapped with the pan-European AdriaArray experiment (2022-2026), a broader initiative aimed at improving the seismic imaging of the central Mediterranean (Kolínský et al., 2025). While this manuscript concentrates solely on FXLand data and operations, the complementary nature of the two experiments may enable joint analyses in future regional-scale studies.

A preliminary description of the FXLand deployment was presented in Margheriti et al. (2024), an INGV Technical Report written in Italian. The present article builds significantly on that documentation by providing, to the international community, new analyses, quantitative evaluation of station performance, and the integration of the FXLand dataset into the INGV real-time surveillance system and the Italian Seismic Bulletin (BSI).

Finally, the integration of data from the FXOBS offshore network, once fully processed and validated, is expected to further enhance the detection and location accuracy of offshore earthquakes, contributing to a more complete understanding of seismic processes and active fault systems along the Ionian margin.

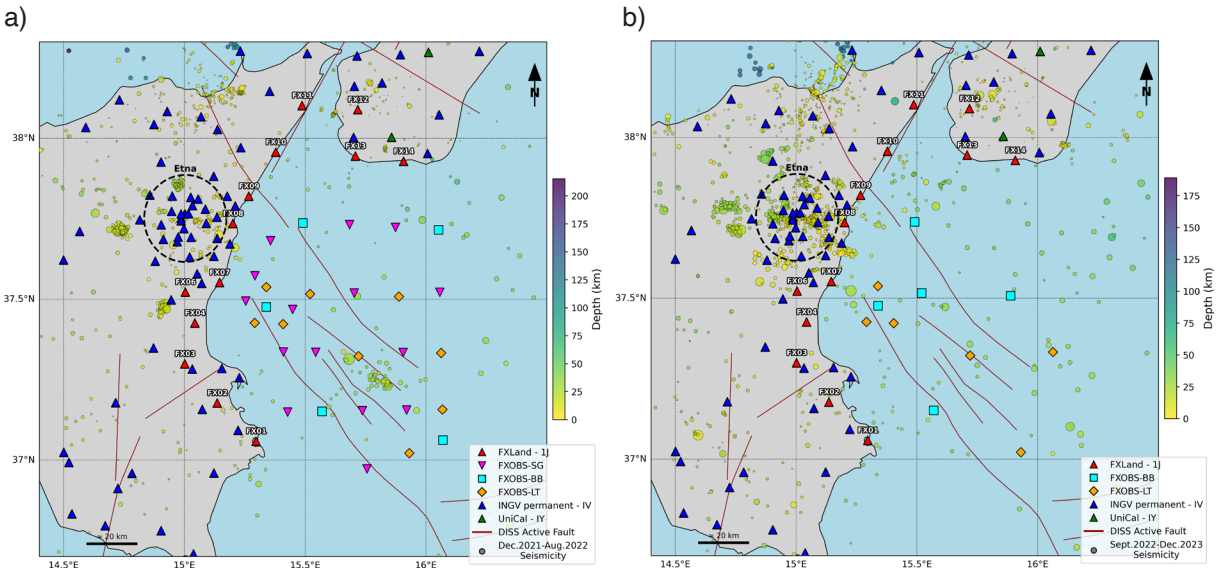

Figure 2. Map showing the configuration of the FXLand onshore (red triangles) and the FXOBS offshore networks (symbols coloured according to instrument type: SG, BB, and LT) during the study period, integrated with the INGV (blue triangles) and UniCal (green triangles) permanent stations. (a) Initial FXOBS deployment (29 instruments) and seismicity between December 2021 and August 2022. (b) Reconfigured FXOBS array (11 instruments) and seismicity between September 2022 and December 2023. FXLand stations remained unchanged throughout the experiment. Seismicity is shown as coloured circles scaled by magnitude and coloured by depth. Active faults (red lines) are from the DISS 3.3.1 database (DISS Working Group, 2025).

2. The FXLand network: strategic integration and instrumental design

The target area, encompassing the Ionian margin and eastern Sicily, is currently monitored by several permanent seismic networks. These include the Italian Seismic Network (RSN; IV network code), the Mediterranean Seismic Network (MedNet; MN network code), and the University of Calabria network (UniCal; IY network code). Among these, the UniCal IY.CNDF station in Condofuri (Reggio Calabria) played a key role in the southernmost part of the study area. This station was fully integrated into the INGV acquisition system at the time of the 1J network activation. Such integration further enhanced the coverage in southern Calabria and contributed to the overall improvement of regional seismic monitoring.

The FXLand temporary network was explicitly designed to complement this existing infrastructure through the installation of 13 broadband seismic stations (labelled FX01 to FX14) along the Ionian coasts of Sicily and Calabria, strategically placed to improve coastal coverage in an area characterized by highly heterogeneous crustal structures and active offshore fault systems described in Section 1.

Although the FXLand stations reduce the distance to offshore sources and densify coverage along the coast, their geometry alone cannot resolve the large azimuthal gap inherent to land-only monitoring of earthquakes occurring beneath the Ionian Sea. Existing permanent and temporary stations occupy a single continental sector to the west of the epicentral region, producing azimuthal gaps typically exceeding 220-260°, which limits both detection threshold and depth resolution, particularly for submarine events (Kissling et al., 1994; Husen and Smith, 2004; Vassallo et al., 2012). For this reason, FXLand was designed as a coastal complement to the offshore FXOBS deployment of 29 OBS. Only the joint use of FXLand and FXOBS can effectively close the azimuthal gap and enable high-precision, land-sea earthquake locations; however, the integrated analysis of FXLand-FXOBS data is beyond the scope of this study. Instead, this work focuses on the onshore array and its contribution to national seismic surveillance and monitoring.

2.1 Planning and equipment of the onshore network: a collaborative approach

The successful implementation and operation of the FXLand network were managed by a dedicated Working Group (WG), including personnel from INGV (with ONT as the lead organization) and UniCal (https://progetti.ingv.it/it/focus, last accessed February 2025). The WG oversaw the entire project life cycle, covering both technical and scientific aspects, from careful planning and design of the temporary network to managing data acquisition and disseminating results. Its responsibilities included organizing field surveys, supervising equipment inventory, coordinating installation and maintenance, and ultimately overseeing the removal of the stations. Following the planning phase, each temporary station was configured to ensure robustness, rapid deployment, and reliable operation. The instrumentation relied on assets coordinated through INGV's Mobile Network Commission (CoReMo), which manages requests and allocates equipment from the ONT's mobile seismic network store (Moretti et al., 2010). For FXLand, this included Reftek 130 digitizers paired primarily with Trillium Compact 120s broadband sensors, alongside two stations using short-period Lennartz-Electronic LE-3D/5s velocimeters. UniCal contributed two stations equipped with SL06 digitizers and SS08 60s sensors from Sara Electronic instruments (https://www.sara.pg.it/). Each site also included a GPS antenna for precise timing and a low-power communication system, enabling near-real-time data transmission whenever feasible.

Site suitability was carefully evaluated considering factors critical for real-time operation. This included reliable UMTS/LTE signal coverage for data transmission, as well as the availability of a stable power supply, provided either by solar panels with long-life batteries or through the local electrical network (Table 1). To standardize field operations and minimize configuration errors, all components were pre-assembled into modular kits, allowing each station to be rapidly activated shortly after site selection.

A distinctive aspect of the deployment was placing the 13 stations along the coast, deliberately accepting higher levels of anthropogenic noise in order to improve the network coverage for monitoring offshore seismicity. Instrument security and rapid troubleshooting were facilitated through the 2019 memorandum of understanding between INGV and the "Arma dei Carabinieri" (Italy's national Gendarmerie) which allowed stations to be hosted within secure Carabinieri headquarters (Fig. 3). In several areas, temporary stations were located near existing permanent INGV sites due to the location of the headquarters along the Ionian coast. The proximity to existing permanent stations thus provides a notable methodological advantage for future studies, as this configuration allows for direct waveform comparison and holds the potential to yield valuable information on local site effects, a well-established procedure in seismological practice (e.g., Cogliano et al., 2021; Bruni et al., 2022).

2.2 Network operation and maintenance: ensuring data quality and completeness

Following the planning and equipment strategies described in Section 2.1, all FXLand temporary stations underwent thorough preparatory testing before deployment. Comprehensive huddle tests were conducted at the INGV offices in Rome, Nicolosi (Catania), and Rende (Cosenza) between November 25 and December 2, 2021,

Table 1. Main characteristics of the FXLand temporary seismic stations deployed along the Ionian coasts of Sicily and Calabria, including sensor type, site setting and installation geometry (sensor buried or not-buried). All stations transmitted data in real time to the INGV data center via UMTS.

Station Name	Location	Start time	End time	Latitude (°)	Longitude (°)	Elevation (m)	Equipment	Sampling (Hz)	Power	Installation site settings	Sensor installation
FX01	Siracusa, Ortigia (SR)	22/12/2021 08:00:00	02/02/2023 23:59:00	37,0586	15,2964	50	Reftek 130S + Trillium Compact 120s	100	Mains	Sensor placed directly on the floor of the Carabinieri headquarters courtyard; paved surface	Not buried
FX02	Melilli (SR)	22/12/2021 08:00:00	02/02/2023 23:59:00	37,1775	15,1357	272	Reftek 130S + Trillium Compact 120s	100	Mains	Sensor installed on the floor of a garage at ground level within the Carabinieri headquarters.	Not buried
FX03	Lentini (SR)	22/12/2021 08:00:00	02/02/2023 23:59:00	37,2992	15,0017	34	Reftek 130 + Trillium Compact 120s	100	Solar	Sensor buried in fill soil within the Carabinieri headquarters garden, close to a road	Buried (~40 cm depth)
FX04	Catania, La Playa (CT)	22/12/2021 08:00:00	02/02/2023 23:59:00	37,4261	15,0431	10	Reftek 130 + Trillium Compact 120s	100	Solar	Sensor buried in alluvial sediments and covered with volcanic sand within the headquarters garden	Buried (~50 cm depth)
FX06	Misterbianco (CT)	22/12/2021 08:00:00	02/02/2023 23:59:00	37,5223	15,0037	118	Reftek 130S + Lennartz 5s	100	Mains/ Solar	Sensor installed at ground level in the external parking area of the Carabinieri headquarters; paved surface.	Not buried
FX07	Aci Castello (CT)	22/12/2021 08:00:00	02/02/2023 23:59:00	37,5521	15,1452	49	Reftek 130S + Trillium Compact 120s	100	Mains	Sensor installed on the floor of a boiler room inside the Carabinieri headquarters	Not buried
FX08	Riposto (CT)	22/12/2021 08:00:00	02/02/2023 23:59:00	37,7352	15,2006	13	Reftek 130 + Trillium Compact 120s	100	Solar	Sensor buried in fill soil within the Carabinieri headquarters garden	Buried (~40 cm depth)
FX09	Giardini Naxos (ME)	22/12/2021 08:00:00	02/02/2023 23:59:00	37,8203	15,2664	23	Reftek 130 + Trillium Compact 120s	100	Mains	Sensor buried in fill soil within the Carabinieri headquarters garden.	Buried (~40 cm depth)
FX10	Santa Teresa di Riva (ME)	22/12/2021 08:00:00	10/03/2023 09:45:00	37,9570	15,3777	29	Reftek 130 + Trillium Compact 120s (till 09/03/2022)/ Lennartz 5s (from 10/03/2022)	100	Mains	Sensor installed at ground level outside the Carabinieri headquarters; tiled surface.	Not buried
FX11	Santo Stefano Medio (ME)	22/12/2021 08:00:00	17/04/2023 12:00:00	38,1019	15,4868	19	Reftek 130 + Trillium Compact 120s	100	Mains	Sensor installed on the floor inside a records storage room of the Carabinieri headquarters; tiled floor.	Not buried
FX12	Cataforio (RC)	22/12/2021 08:00:00	14/06/2023 23:59:00	38,0895	15,7176	253	Sara SL06 + Sara SS08 60s	100	Mains	Sensor installed on the floor inside a ground-floor technical room of the Carabinieri headquarters; tiled floor.	Not buried
FX13	Montebello Jonico, Saline (RC)	22/12/2021 08:00:00	18/04/2023 12:00:00	37,9945	15,7075	21	Reftek 130 + Trillium Compact 120s	100	Mains	Sensor installed on the floor inside a basement garage of the Carabinieri headquarters; tiled floor.	Not buried
FX14	Bova Marina (RC)	22/12/2021 08:00:00	14/06/2023 23:59:00	37,9286	15,9070	21	Sara SL06 + Sara SS08 60s	100	Mains	Sensor installed on the floor inside a basement garage of the Carabinieri headquarters; tiled floor.	Not buried

Figure 3. Examples of station installations at representative sites.

with the aim of identifying and resolving potential configuration issues related to the sensors, digitizers, and the ReMoNET acquisition server. For instance, the Rende group installed and tested station FX13 on November 24, 2021, while the UniCal stations (FX12 and FX14) were powered on the same day, with their data streams made available via SeedLink and successfully acquired by the dedicated server. In Catania, four stations (FX05, FX07, FX08, FX09) were tested starting November 26, 2021, at 10:00 AM, allowing the operators to immediately detect issues such as a damaged router at FX07, which initially prevented data transmission. These preparatory procedures ensured that the deployment could be carried out efficiently and with minimal risk of configuration errors, thereby maximizing operational reliability from the outset.

The field installation phase took place between December 13 and 18, 2021, with data archiving beginning on December 22, 2021, at 00:00 UTC. By the launch date, 13 of the 14 planned stations had been successfully deployed. The remaining station, FX05, was excluded due to logistical and instrumental issues: although the sensor and digitizer performed adequately during testing, a persistent modem configuration conflict prevented the reliable real-time transmission required for operational integration. Network management and maintenance were organized on a regional basis: the Catania office supervised the Sicilian sites, while the Rende office (ONT and Seismology Laboratory of UniCal) managed the Calabrian stations. This decentralized organization allowed for rapid responses to operational issues and continuous monitoring of station performance.

A key component of network operation was the ReMoNET acquisition server interface, which provided operators with comprehensive remote diagnostics. In real time, ReMoNET displayed several critical operational parameters, including internal RAM status, acquisition activity, transmission protocol configuration, and the health of both internal and external power supplies. The system also monitored local memory usage, offering detailed information on data volumes stored on the internal memory cards, essential for preventing overwriting of unrecovered data during telemetry outages. These functionalities allowed operators to prioritize field interventions when the risk of data loss increased.

The importance of these checks became evident during the first days of operation. FX07, for example, remained offline until December 21, 2021, due to a missing Ethernet write-enable configuration flag. Additionally, real-time waveform inspection revealed off-scale signals at FX09 and FX10, indicating poor sensor levelling and prompting on-site intervention by OE personnel.

Figure 4 shows the daily operational percentages of all the stations during the main functioning period of the 1J network where light vertical stripes indicate interruptions in data transmission. Several issues affected individual stations, such as temporary power supply limitations (e.g., FX06 initially powered by solar panels before subsequent connection to the electrical grid) modem malfunctions (FX03 and FX10), and intermitted GPS antenna connectivity problems (FX08 and FX13). Despite these challenges, the network achieved an overall data recovery rate consistently above 80% throughout the main operational period.

An important contribution to network continuity came from the personnel stationed at the Carabinieri headquarters hosting several sites, who provided prompt support during power outages, solar panel shadowing, and GPS obstructions caused by vegetation. Their timely interventions helped stabilize station performance and minimize data loss.

The decommissioning of the temporary network began in early 2023 and was conducted in three phases. An initial group of nine stations was deactivated in early February, followed by the staged removal of the remaining stations between April and June, ensuring orderly closure and recovery of the temporary network assets.

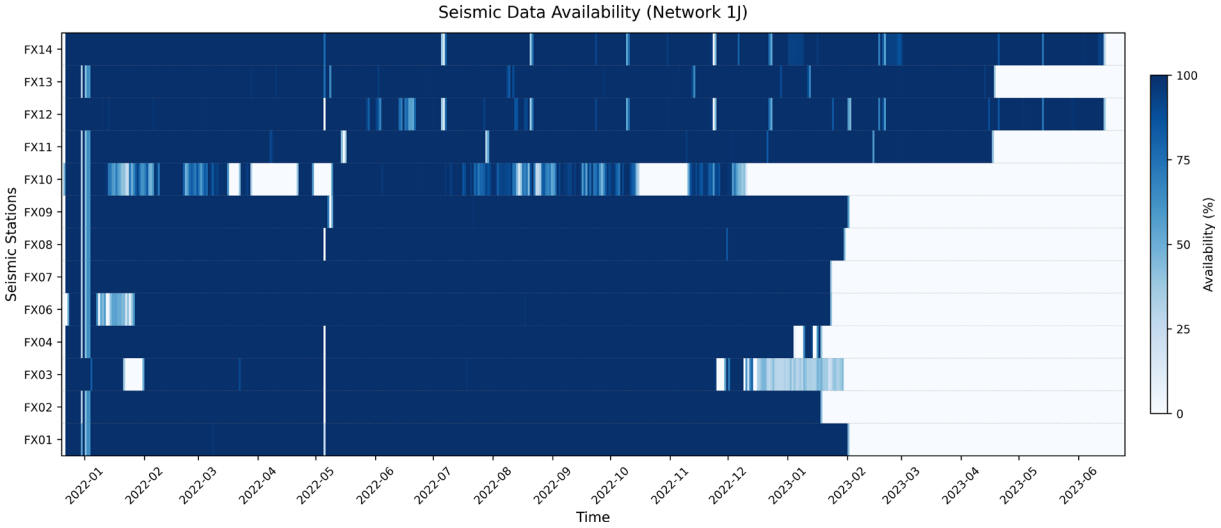

Figure 4. Daily operational percentages of all the stations during the main functioning period of the 1J network.

3. Data quality, archiving, and sharing

3.1 Data quality assessment

The quality of the seismic data recorded by the FXLand temporary network was systematically evaluated throughout its operational period to assess its suitability for real-time surveillance and subsequent analyses. Given the predominantly coastal and urban locations of the stations, elevated ambient noise levels were expected, particularly at high frequencies.

Station noise characteristics were analyzed using Probabilistic Power Spectral Density (PPSD) analyses (McNamara and Buland, 2004), which provide a statistical description of background seismic noise by combining multiple Power Spectral Density (PSD) measurements over time. The resulting noise distributions were compared with the New Low Noise Model (NLNM) and New High Noise Model (NHNM) defined by Peterson (1993), which represent reference bounds for global seismic noise levels.

PPSD estimates discussed in this section were computed on the vertical components of all stations over the period from June 25, 2022, to July 4, 2022, selected as a representative time window characterized by stable network configuration and continuous data availability across the majority of stations. The analysis was performed on the vertical component, which provides the most robust and directly comparable estimate of ambient seismic noise for data quality assessment and sensor performance evaluation. This choice allows a consistent comparison among sites and sensor types under comparable acquisition conditions. A detailed station-by-station description of PPSD characteristics is provided in Supplementary Material S1.

Generally, in the high-frequency range (approximately 1-50 Hz), most FXLand stations exhibit elevated noise levels consistent with intense anthropogenic activity along the Ionian coast, including, railways, roads traffic, and urban infrastructure. Within this frequency band, the noise distributions generally lie between the NLNM and NHNM, with only rare exceedances of the upper noise model. Focusing on the highest frequencies ($f > 10$ Hz), the PPSD distributions do not show a pronounced bimodal pattern. indicating the absence of a significant disparity between daytime and night-time noise level. This ubiquitous feature across the entire network is typical of densely urbanized areas, where anthropogenic activities maintain a persistently high noise floor regardless of the hour.

At lower frequencies ($f < 1$ Hz), noise characteristics show larger variability among stations and primary reflect differences in sensor types, installation geometry and local site conditions.

To mitigate temperature-related effects on sensor performance, specific mitigation measures were adopted depending on installation geometry. For all not-buried stations, the sensors were insulated using polystyrene beads and protected by a PVC cap with an external cover. For buried installations, thermal insulation was provided by the surrounding soil or, in some cases, by volcanic ash.

Figure 5 illustrates a comparison between stations FX01 and FX11, both equipped with the same broadband sensor (Nanometrics Trillium 120s Compact) and installed in similar coastal settings but characterized by different

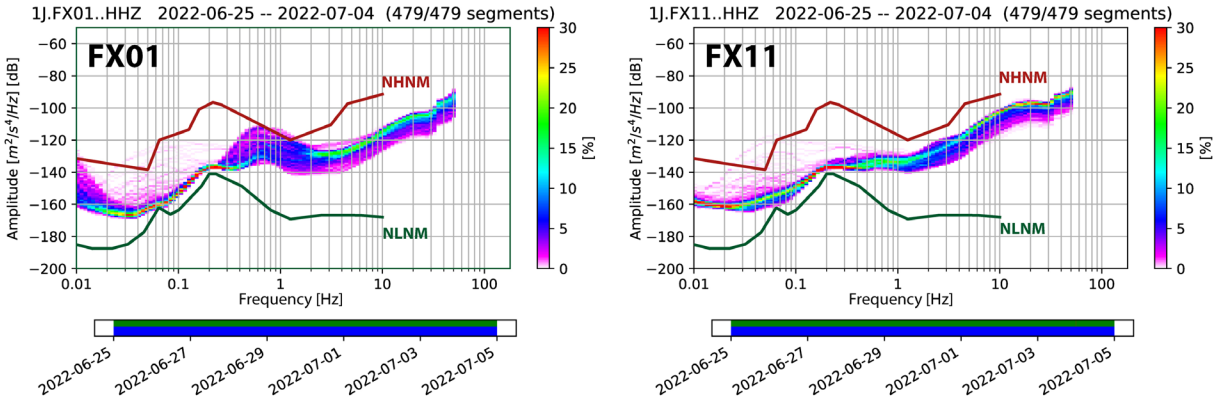

Figure 5. Example of the vertical component PPSD for stations FX01 and FX11. At low frequencies, both stations exhibit relatively low noise levels, approaching the NLNM, whereas at high frequencies, they show elevated noise levels, consistent with the densely urbanized areas.

low-frequency noise behavior. Despite identical instrumentation, the PPSD curves show distinct absolute noise levels below 1 Hz, with FX11 approaching the NLNM more closely than FX01 over the same frequency range, indicating effective sensor thermal insulation and stable coupling conditions even in coastal and urban environments.

At very low frequencies ($f < 0.1$ Hz), FX11 displays a narrow and stable noise plateau, whereas FX01 is characterized by slightly higher and more dispersed noise levels. This contrast highlights differences in long-period ($T > \sim 10$ s) recording stability under comparable sensor configurations and environmental settings.

Considering the instrumental diversity of the FXLand network, which includes broadband sensors (Trillium Compact 120 s and Sara SS08 60 s) as well as extended-band short-period sensors (Lennartz LE-3D/5 s), differences in noise behavior at long periods cannot be attributed solely to local conditions.

These differences also reflect intrinsic variations in sensor response, particularly at periods longer than approximately 10 s, where corner frequency and instrumental self-noise become dominant.

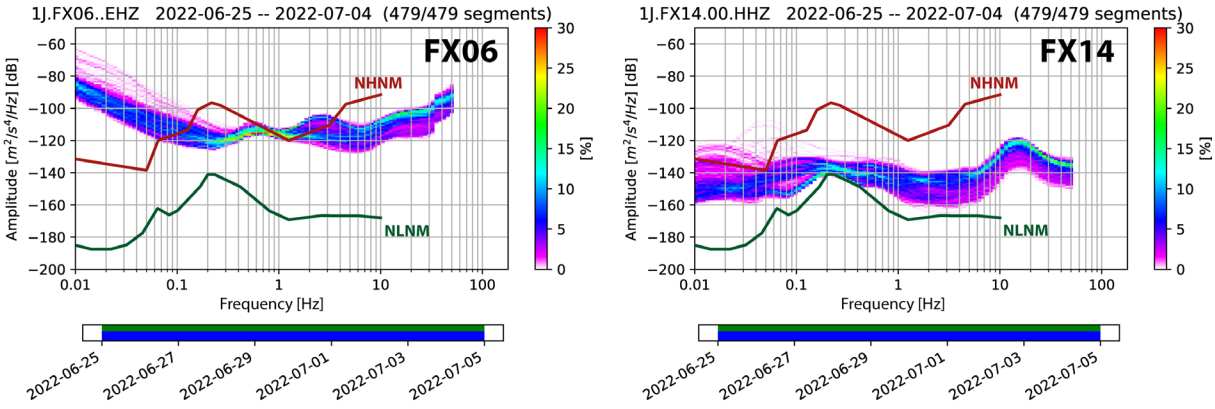

Figure 6. Vertical component PPSD for stations FX06 (Lennartz Le3d-5s sensor) and FX14 (Sara SS08 60 s broadband sensor). The FX06 shows a pronounced increase in noise below ~0.2 Hz, reflecting electronic self-noise, while FX14 exhibits higher low-frequency noise compared to other broadband stations. The effect of sensor response on noise characteristics is illustrated in Fig. 6, which compares the PPSD of station FX14, equipped with a Sara SS08 60 s broadband sensor, with that of station FX06, equipped with and an extended-band Lennartz Le3d-5s short-period sensor. The spectral curves clearly highlight the technical limitations associated with different sensor types. Specifically, FX06 station exhibits a pronounced increase in the noise floor at frequencies below ~0.2 Hz. This behavior is directly attributed to the instrumental self-noise of the electronics when the sensor operates beyond its nominal corner frequency, representing an intrinsic limitation of the extended-band short-period instruments at long periods. In contrast, FX14 station exhibits a more stable low-frequency response, consistent with the expected performance of a broadband sensor. Although its PSD levels are systematically higher than those recorded at other broadband stations in the network, likely reflecting local site condition or sensor coupling, the overall noise level remains below the New High Noise Model (NHNM) across the analyzed frequency range

3.2 Data management, archiving and accessibility

The FXLand experiment produced a continuous, real-time seismic dataset designed to support both operational monitoring and scientific analyses. All waveform data recorded by the temporary network were automatically integrated into INGV acquisition system and subsequently archived at the Italian node of the European Integrated Data Archive (EIDA; Danecek et al., 2021), operating within the international FDSN data-distribution framework. Data are stored in the Standard for the Exchange of Earthquake Data (SEED) format and are freely accessible to the scientific community through the EIDA web services (https://eida.ingv.it).

Before archiving, standard quality-control procedures were applied to verify waveform completeness, timing accuracy, and metadata consistency. These checks included validation of instrument response files, station coordinates, and acquisition parameters to ensure full interoperability within the EIDA and FDSN standards. Following INGV procedures for temporary networks, the FXLand stations were formally registered with the

International Federation of Digital Seismograph Networks (FDSN; https://www.fdsn.org/) and the International Seismological Centre (ISC; https://www.isc.ac.uk/), guaranteeing long-term preservation and worldwide visibility of the data.

In line with the Open Science framework and the FAIR (Findable, Accessible, Interoperable, Reusable) data principles, each FXLand data stream has been permanently identified and registered through a Digital Object Identifier (DOI) issued by the INGV Data Registry (INGV Data Management Office, 2020). This practice ensures persistent accessibility, unambiguous data citation, and interoperability within international data infrastructures.

The publication and management of the FXLand dataset comply with the INGV Data Policy (Puglisi et al., 2018), coordinated by the INGV Data Management Office, which defines institutional guidelines for open access, data citation, and standardization across INGV repositories. To ensure traceability and accurate citation a DOI has been assigned to the FXLand waveform dataset (Moretti et al., 2021), allowing it to be cited independently of this paper and guaranteeing persistent access through the INGV Data Registry. The dataset includes continuous three-component waveform data acquired between December 2021 and June 2023, together with metadata in StationXML format.

The availability of well-documented, openly accessible waveform data represents a key outcome of the FXLand experiment. Beyond supporting the analyses presented in this work, the FXLand waveform archive provides a long-term resource for future investigations of seismicity, crustal structure, and seismic hazard along the Ionian margin.

4. FXLand integration into real-time seismic surveillance and the Bollettino Sismico Italiano: insights from three seismic sequences

4.1 From seismic surveillance to earthquake analysis

The real-time integration of the FXLand temporary station into the INGV seismic surveillance system provide an opportunity to evaluate their operational contribution to routine earthquake monitoring and bulletin production During the deployment period, from December 22, 2021, to June 15, 2023, the INGV seismic surveillance service in Rome detected 214 teleseismic earthquakes with a magnitude greater than 6, as well as 951 local events – three of which had a local magnitude greater than 4.0 – within the area bounded by latitudes 36.75°N-38.3°N and longitudes 14.5°E-16.1°E.

At a later stage, local seismicity was reanalyzed by the analysts of the Italian Seismic Bulletin (BSI, Bollettino Sismico Italiano, https://bsi.ingv.it, last accessed February 2025; BSI Working Group, 2015). Seismic recordings from the RSN stations were integrated with those from the temporary FXLand stations, providing revised P- and S-waves pickings, as well as updated earthquake locations and magnitudes. In addition, low-magnitude events missed by the automatic surveillance system were identified through subsequent waveform inspection and manually reviewed by BSI analysts. Overall, 1,468 earthquakes were located during the experiment (Fig. 7), increasing the number of P pickings from ~10,100 to ~24,300 and the S pickings from ~6,500 to ~14,500 at the stations within the study area. Of these,1,343 P- and 898 S-wave pickings were obtained from the FXLand stations. The increased number of high-quality phase arrivals improved the constraint on hypocentral parameters, especially depth estimates, and reduced location uncertainties.

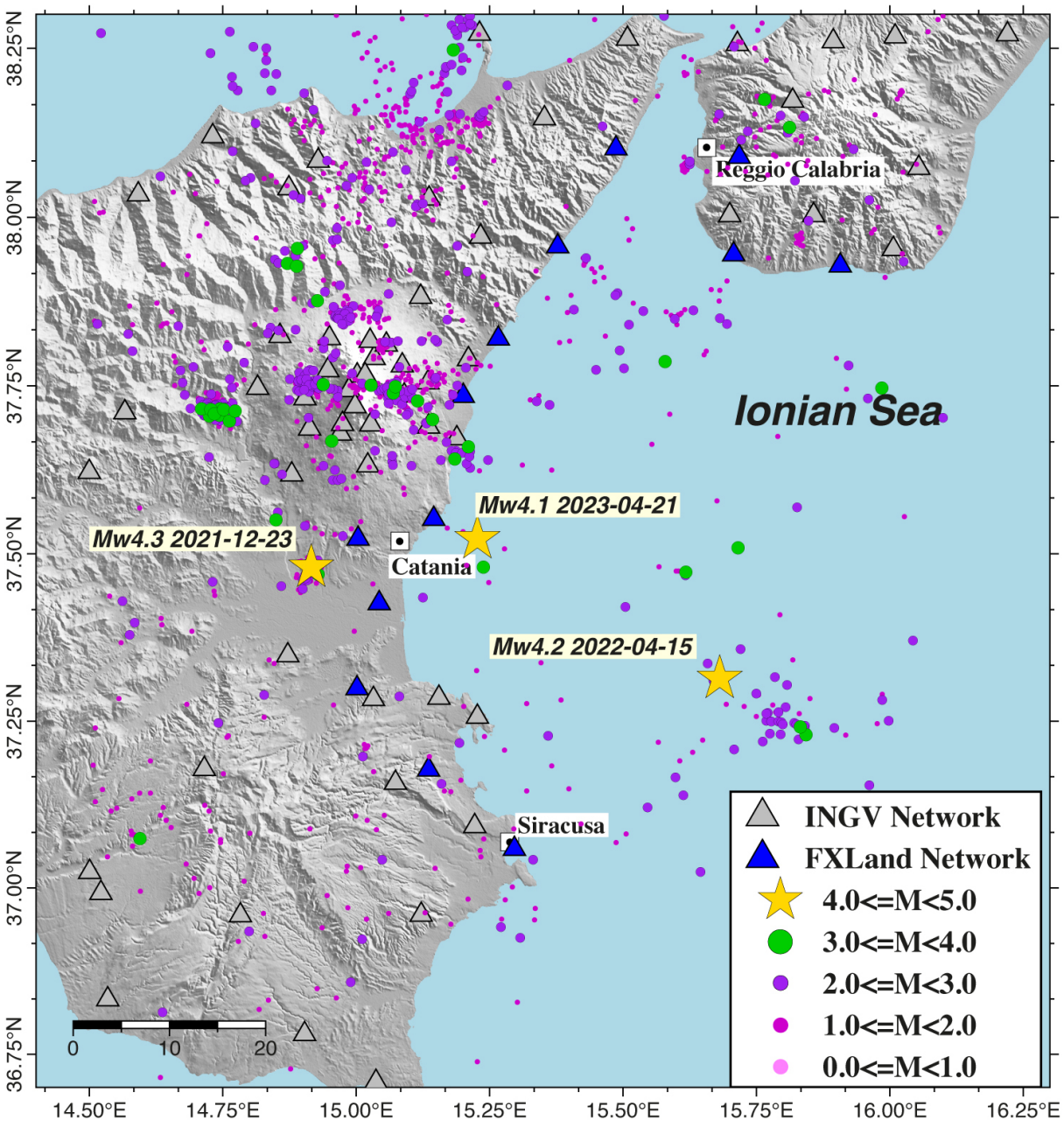

Figure 7. Map view of the seismicity recorded by the integrated network of INGV permanent stations and the FXLand temporary stations from December 22, 2021, to June 15, 2023, and analyzed by the BSI analysts. Earthquakes are represented by symbols scaled by magnitude, as indicated in the inset. Blue and gray triangles represent the temporary FXLand stations and the permanent INGV stations, respectively.

4.2 Impact of the FXLand network on earthquake location quality

To quantitatively assess the improvement in hypocentral location quality provided by the integration of the FXLand network relative to the RSN-only configuration, we performed an earthquake location test on 200 seismic events across Eastern Sicily, Southern Calabria, and offshore areas between the Strait of Messina and the Ionian Sea (Fig. 8). The selected t dataset spans a wide range of magnitudes and includes both onshore and offshore earthquakes. Each event was located under two distinct configurations: (i) using data from the RSN stations only, (ii) using data from the integrated RSN+FXLand stations. To ensure a correct comparison of the results, both inversions were performed using the same location algorithm, inversion parameters tuning, and velocity model.

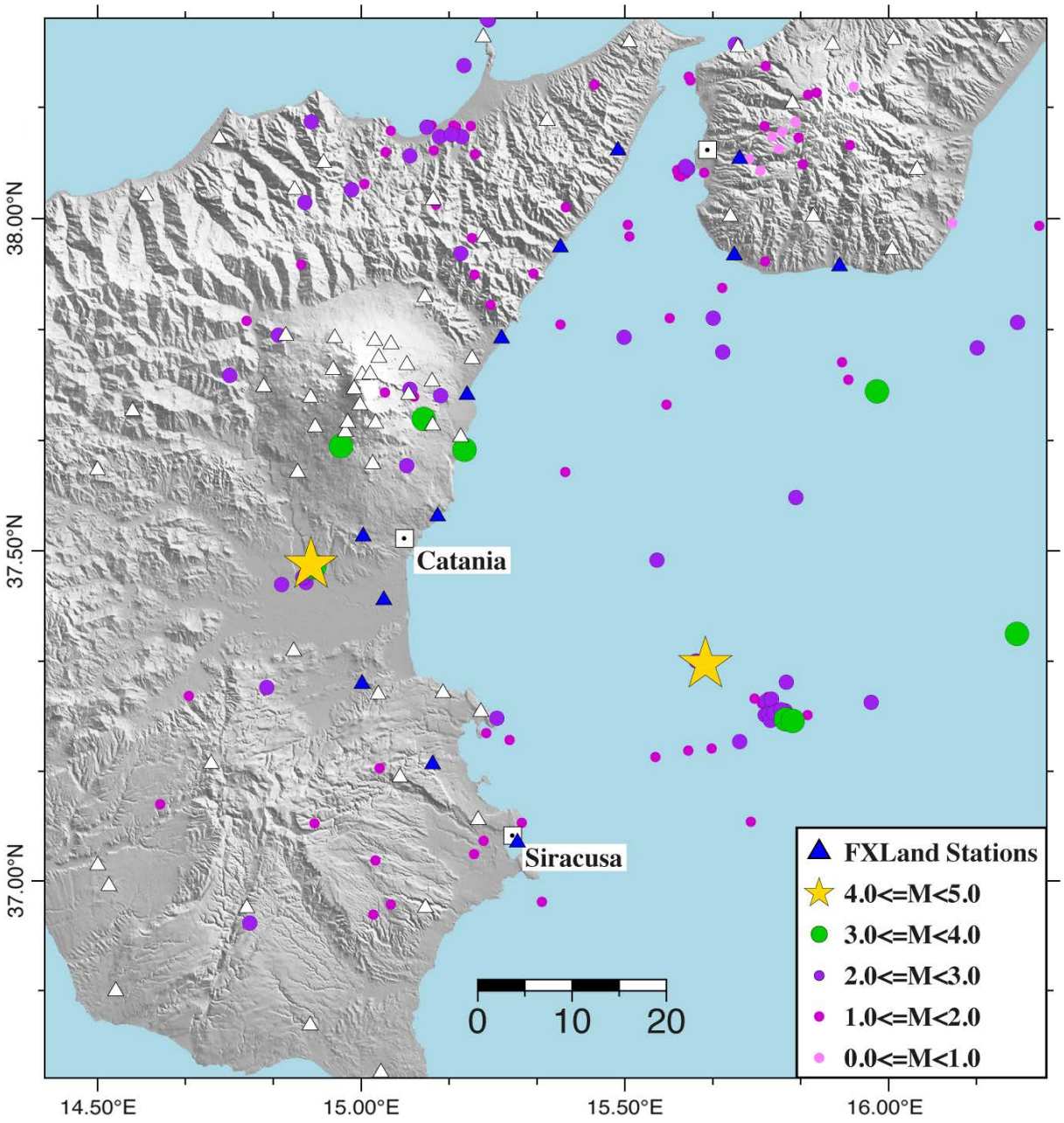

Figure 8. Map of the study area showing the spatial distribution of the 200 events used for the test, scaled by magnitude. Triangles indicate the permanent RSN (white) and the temporary FXLand network (blue). The dataset covers onshore areas in Eastern Sicily and Southern Calabria, as well as offshore zones between the Strait of Messina and the Ionian Sea.

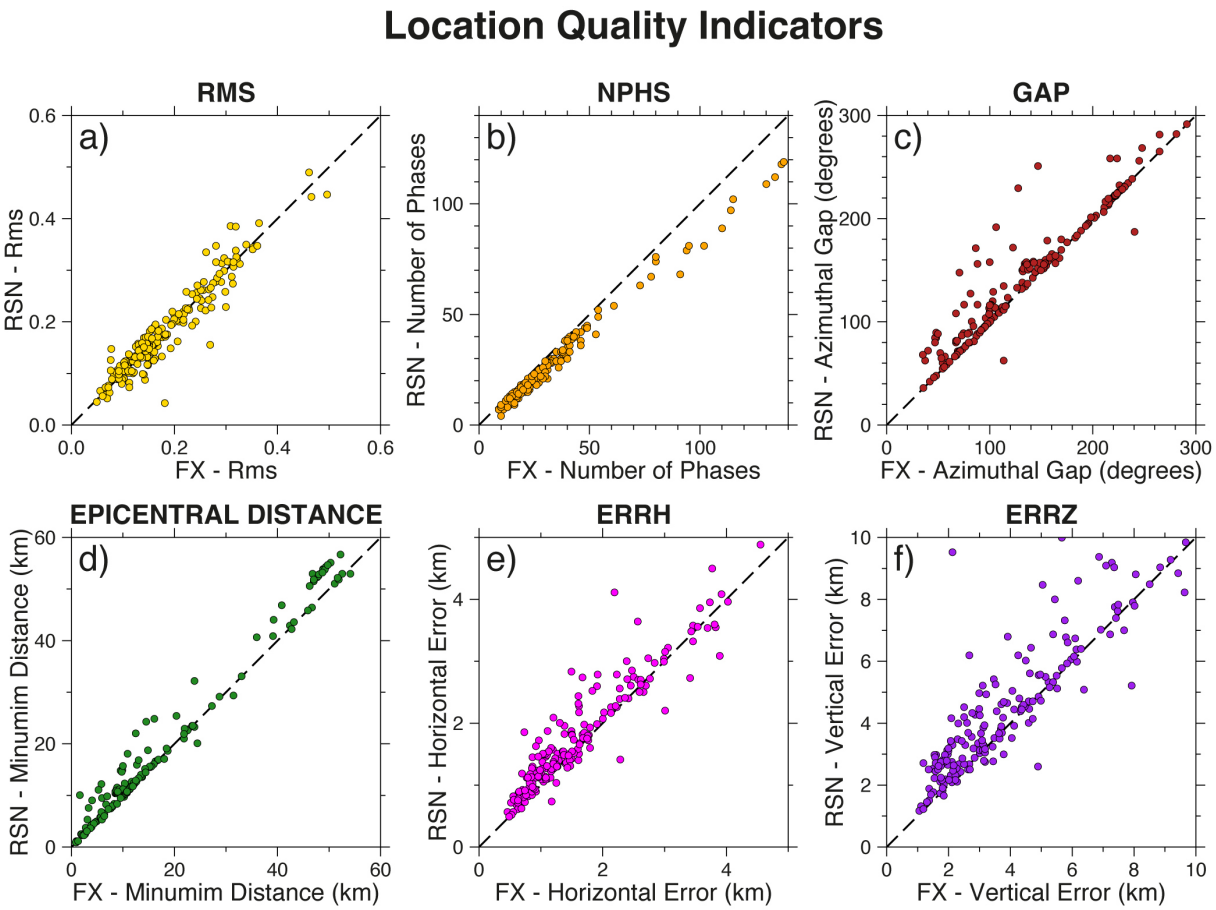

Figure 9. Comparison of location quality indicators between the RSN configuration (y-axis) and the integrated RSN+FXLand network (x-axis). Panels represent: (a) RMS residuals, (b) number of phases (NPHS), (c) azimuthal gap, (d) minimum epicentral distance, (e) horizontal error (ERRH), and (f) vertical error (ERRZ). The dashed line represents the identity line.

Following the relocation process, we analyzed the main location quality indicators, including the Root Mean Square (RMS) residuals, the number of data inverted (P and S phase pickings, NPHS), the azimuthal gap (GAP), the minimum epicentral distance to the nearest station, and both horizontal (ERRH) and vertical (ERRZ) errors. The comparison between the two configurations is illustrated by the scatter plots of Fig. 9, where results from the RSN-only configuration are plotted against those from the integrated configuration, providing an event-by-event comparison of the location-quality indicators. In addition, the overall effect of the FXLand networking integration is summarized in Fig. 10 through the distribution parameter differences. For each earthquake and for each indicator, the difference was calculated as the value obtained using the integrated RSN+FXLand configuration minus the corresponding value obtained using the RSN-only configuration. As a result, negative values generally indicate an improvement in location quality when FXLand stations are included, except for NPHS, for which positive values reflect an increase in the number of inverted phases.

The test demonstrates that the FXLand network integration both optimizes the data fit and reduces the spatial uncertainties. Despite the significant increase in the number of inverted phases (Figs. 9b and 10b), the RMS residuals remain stable, with most events clustering near the identity line in the scatter plot (Fig. 9a) and the corresponding difference distribution centered around zero (Fig. 10a). This demonstrates that integrated data are consistent with the adopted velocity model. This increasing number of phases leads to a more stable and robust hypocenter location inversion and has direct effects on the geometrical indicators. Although the RSN is already dense in this area of Sicily, the distribution of FXLand stations along the coast provides improved azimuthal coverage and closer station-event distances, particularly for onshore and offshore earthquakes.

This effect is clearly visible in the azimuthal gap indicator. In Fig. 9c, many events shift above the identity line, indicating a drastic reduction in the azimuthal gap when FXLand stations are included, which is essential

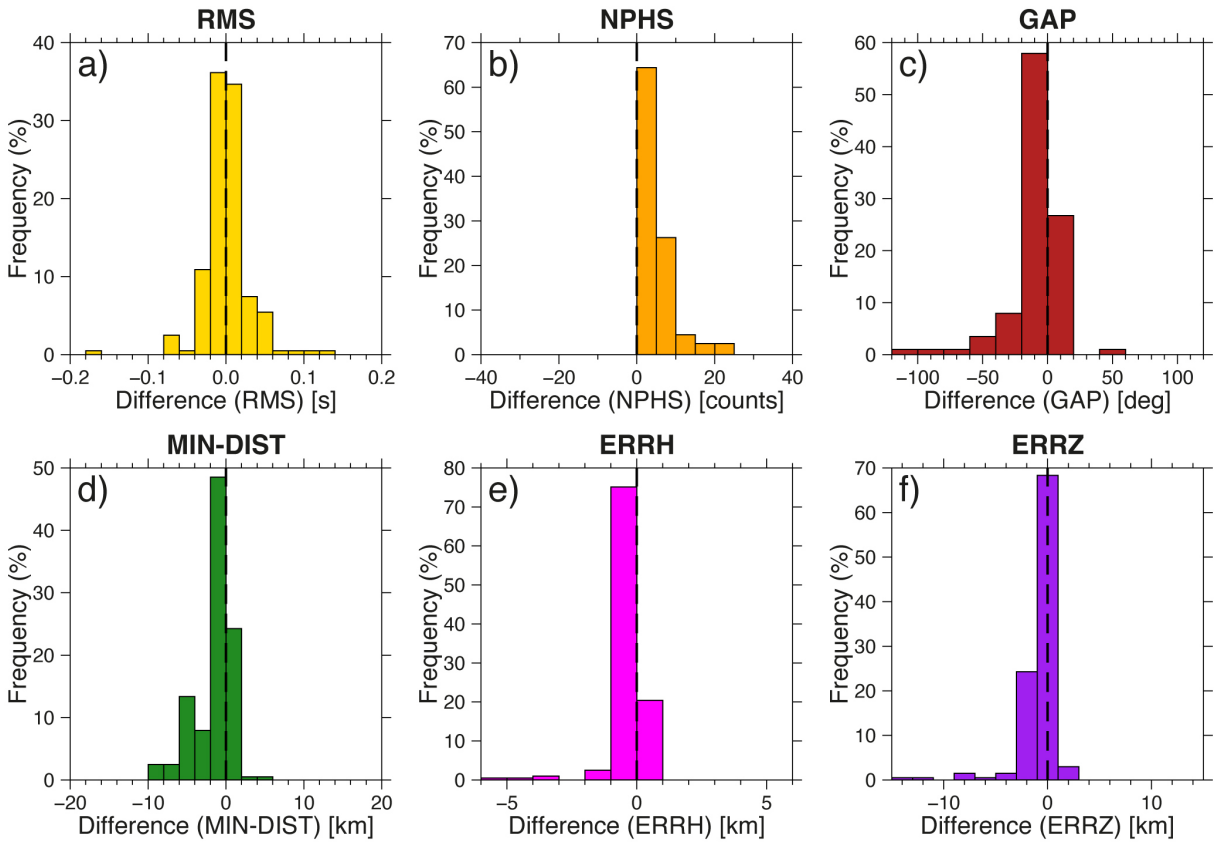

Figure 10. Statistical distribution of the differences for the location quality indicators. Histograms show the frequency of variation, calculated as the value from the integrated FXLand configuration minus the RSN-only value, for: (a) RMS, (b) NPHS, (c) azimuthal gap, (d) minimum epicentral distance, (e) ERRH, and (f) ERRZ.

for ensuring the robustness of the epicentral solution. The corresponding difference distribution of the azimuthal gap (Fig. 10c) shows average variations of approximately 20° and, in several cases, exceeds 50°. Simultaneously, we observe a clear reduction in the minimum epicentral distance to the nearest station (Figs. 9d and 10d), a parameter representing a key parameter for the accurate estimation of hypocentral depth. This reduction, affecting a large portion of the dataset (Fig. 10d), ranges from average values of 2-3 km up to a maximum of 10 km, confirming that network densification with FXLand stations allowed for the detection of events with stations much closer to the epicenter compared to the RSN alone.

This improved network geometry directly translates into a narrowing of formal uncertainties. Both the horizontal (ERRH) and vertical (ERRZ) errors exhibit a shift toward lower value for the integrated RSN+FXLand configuration (Figs. 9e-f and 10e-f). The histograms show a predominance of negative differences, indicating that epicentral and depth uncertainties decrease for a large part of the dataset when the FXLand stations are included.

4.3 Revealing low-magnitude earthquakes via Template Matching

To enhance the observed seismicity in the Ionian Sea region and better constrain the detection of low-magnitude earthquakes, we applied a Template Matching (TM) technique (Gibbons and Ringdal, 2006; Shelly et al., 2007) to the integrated RSN+FXLand dataset. The aim was to identify additional low-magnitude events present in the continuous recordings but not included in the real-time analyses of the INGV surveillance system and the Italian Seismic Bulletin (BSI) catalogs. This approach increases the number of detected low-magnitude earthquakes with respect to routine operational catalogs and allows a more detailed characterization of seismic activity.

Starting from the manually revised catalog, separate P- and S-wave templates were constructed using stations contributing to the event locations within a defined distance radius. Template lengths were set to 0.8 s for P-waves and 1.2 s for S waves, starting 0.1 s before the picked arrival time. To maximize the signal-to-noise ratio,

vertical-component waveforms from both templates and continuous data were preprocessed using a four-poles Butterworth filter between 2 and 15 Hz. Cross-correlation was performed independently for P and S phases using sliding windows with 50% overlap, and a detection was declared when at least three P-wave and three S-wave correlations exceeded a threshold of 0.6. This procedure enabled the identification of earthquakes with magnitudes close to zero that were not detected by routine processing.

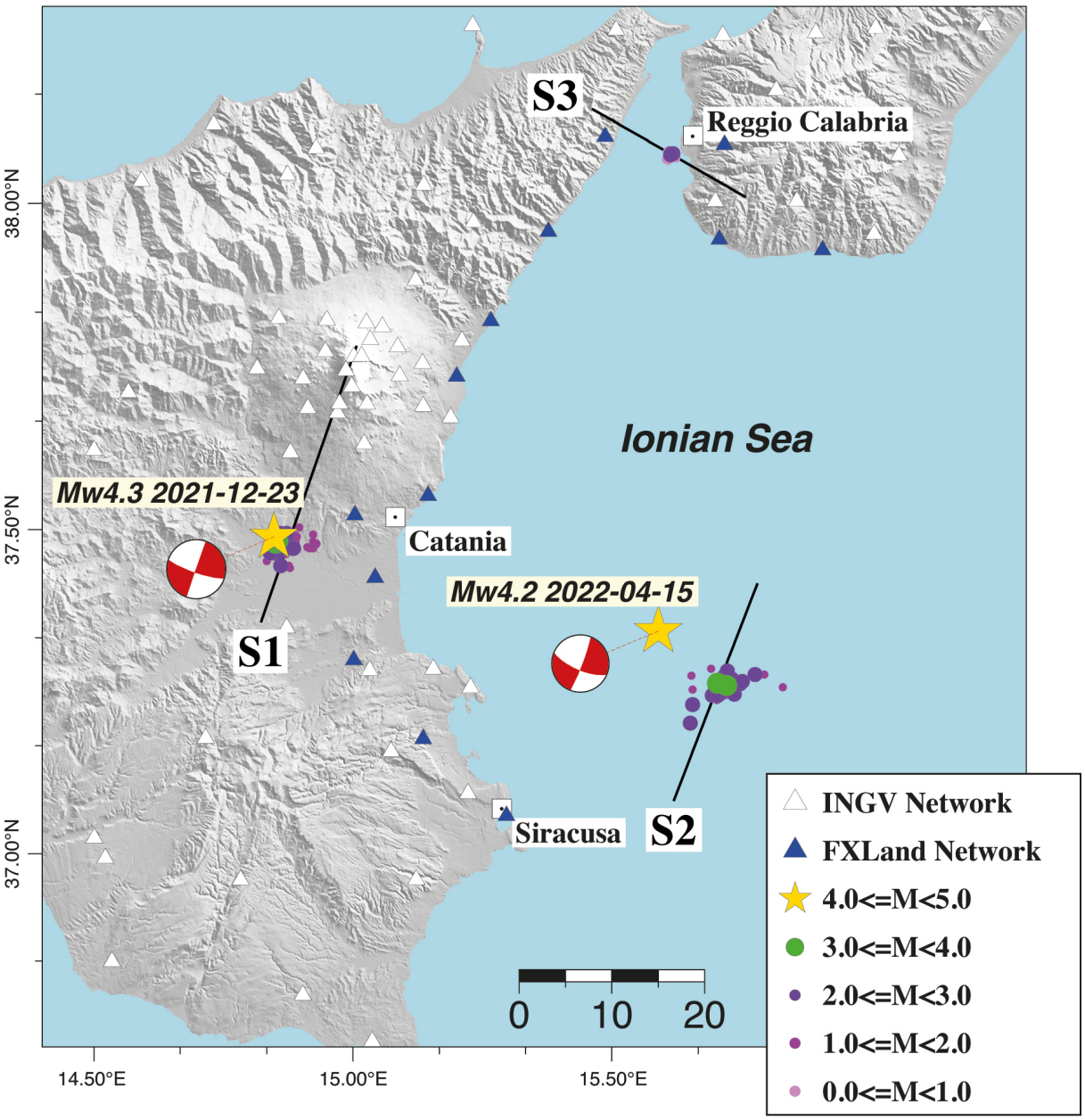

Figure 11. Map view of the three seismic sequences analyzed in this study (S1, S2, and S3), showing the spatial distribution of earthquakes detected using the Template Matching technique. Earthquakes are colored by magnitude class, as indicated in the legend; yellow stars mark the mainshocks ($4.0 \leq M < 5.0$). White triangles represent permanent INGV seismic stations, while blue triangles indicate temporary FXLand stations. Black lines indicate the traces of the vertical cross-sections shown in Figs. 12, 13, and 14 for sequences S1, S2, and S3, respectively. For sequences S1 and S2, the section orientations are chosen approximately perpendicular to the strike of the probable activated structures, inferred from the spatial distribution of seismicity and available focal mechanism information. For sequence S3, where no moment tensor solution is available, the section is oriented perpendicular to the strike of the dominant fault reported in the DISS database, and representative of the main seismogenic structure in the area

To illustrate the effects of the TM analysis and the contribution of the FXLand onshore network, we focus on three representative seismic sequences (Fig. 11), selected within the framework of the FOCUS project and characterized by different tectonic settings and monitoring conditions. All detected earthquakes were relocated using the NonLinLoc program (Lomax et al., 2000, 2014), which calculates hypocentral locations based on a probabilistic approach and a nonlinear inversion algorithm. Hypocentral locations were computed using a regional 1D velocity model suitable for the study area (Latorre and Di Stefano, 2024; Pastori et al., 2020).

For each of the three analyzed seismic sequences, vertical cross-sections were defined to investigate the spatial and depth distribution of the relocated events. The orientation of the sections was selected on the basis of the available geological and seismotectonic information. For sequences S1 and S2, the sections were oriented approximately perpendicular to the strike of the probable activated structures, as inferred from the spatial distribution of seismicity and, where available, focal mechanism information. For sequence S3, where no moment tensor solution was available, the section orientation was chosen perpendicular to the strike of the dominant fault plane reported in the DISS database for the Messina Strait area (see Fig. 2).

Sequence 1: Motta Sant'Anastasia (Eastern Sicily)

The first seismic sequence began on December 23, 2021, with a mainshock of ML 4.3, approximately 6 km southwest of Motta Sant'Anastasia (Catania). During the sequence, the real-time seismic surveillance service located 52 aftershocks, with a minimum magnitude of ML 1.17, while the subsequent BSI review increased the catalog to 80 events (approximately 53% more than the surveillance catalog) and lowered the minimum magnitude to ML 1.13.

The application of the TM analysis further increased the number of detected earthquakes to 128, corresponding to more than twice the number identified by the surveillance service and about approximately 60% more than those included in the BSI catalog. The minimum detected magnitude was reduced to ML 0.63.

The relocated seismicity delineates a well-defined cluster within an area approximately 5x5 km^2. In terms of hypocentral depth, seismicity is mainly concentrated between 15 and 20 km, with the Mw 4.3 mainshock located at about 21 km depth (Fig. 12a). The corresponding magnitudes distribution (Fig. 12b) shows that most events have local magnitude between 1.0 and 2.0, consistent with a typical aftershock sequence following a moderate crustal earthquake in eastern Sicily.

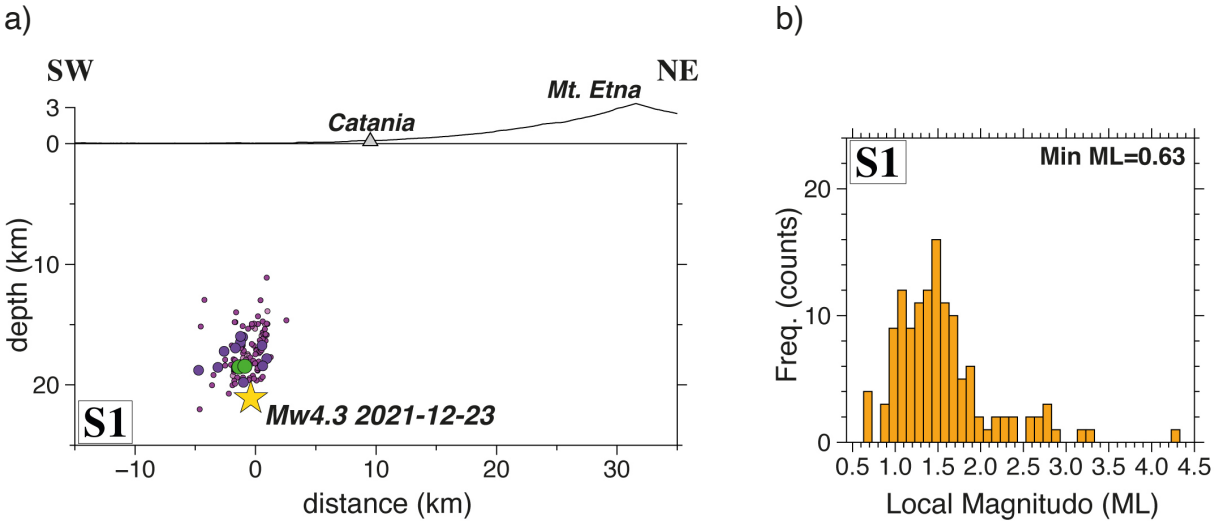

Figure 12. Relocated seismicity of the Motta Sant'Anastasia sequence (S1) obtained from the Template Matching catalog. (a) Vertical cross-section along the SW-NE direction showing the spatial and depth distribution of the earthquakes. (b) Magnitude histogram of the relocated events, showing that most earthquakes have local magnitudes between about 1.0 and 2.0, with a minimum magnitude of ML 0.6.

Sequence 2: Ionian Sea offshore sequence

The second seismic sequence occurred offshore in the Ionian Sea between 6 February and 27 April 2022. Routine real-time processing identified 30 earthquakes during this period, with a minimum recorded local magnitude of

ML 1.2. Seismic activity was most intense between February and March, whereas the Mw 4.2 event on April 15, 2022, appears spatially and temporally isolated from the main cluster.

The relocated events exhibit a scattered spatial distribution and span a wide range of hypocentral depths, approximately between 25 and 45 km (Fig. 13a). This dispersion reflects the offshore location of the sequence, located about 20 km from the coast, which results in unfavorable station geometry and limits the resolution achievable using land-based stations only.

The magnitude distribution of the events TM-detected (Fig. 13b) is dominated by earthquakes with local magnitudes between about 1.5 and 2.3 and the minimum detected event reaches ML 1.2. Although the application of the TM technique increases the number of low-magnitude events, the limited azimuthal coverage and large epicentral distances prevents a robust characterization of the activated structures. This sequence therefore highlights the intrinsic limitations of land-only seismic networks for offshore seismicity and underscores the importance of integrating ocean-bottom seismometer data, such as those from the FXOBS network, to improve both detection capability and hypocentral resolution.

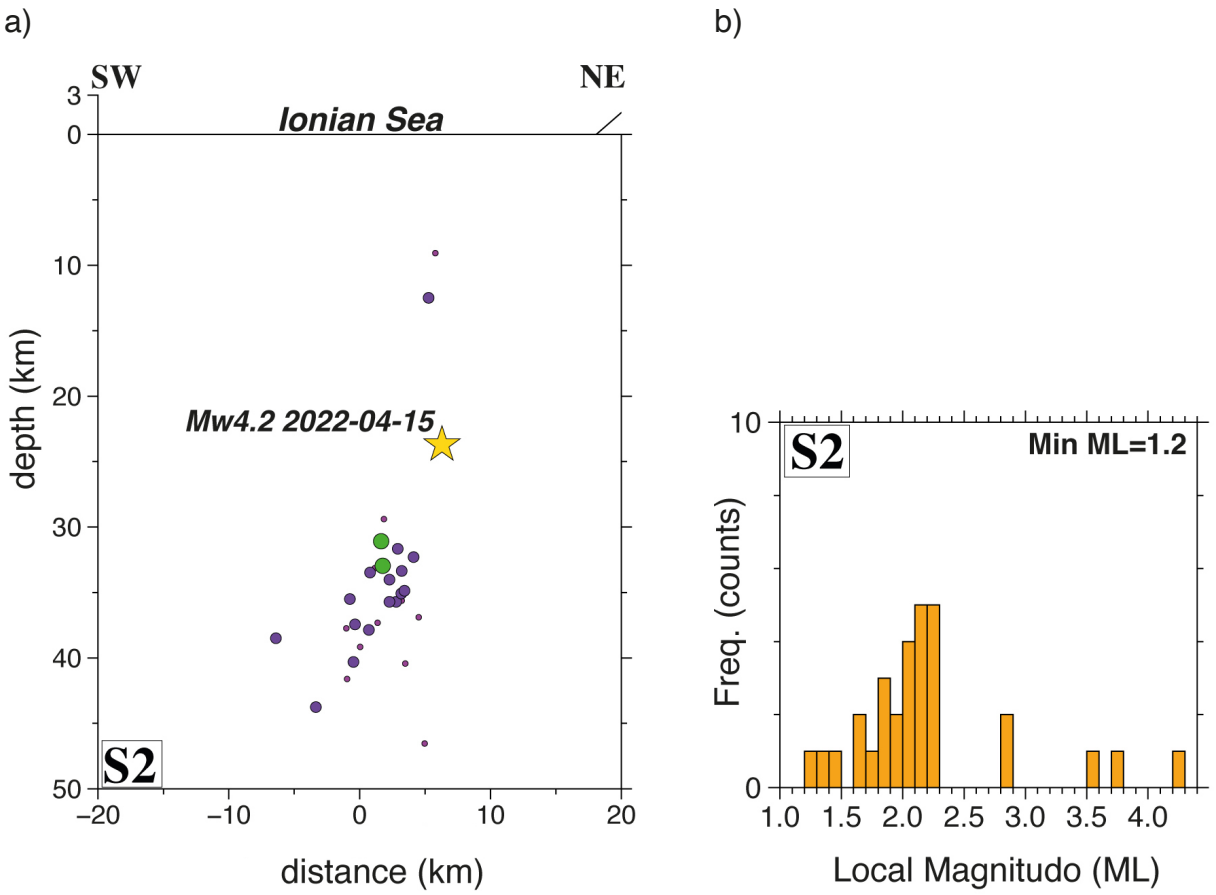

Figure 13. Relocated seismicity of the offshore Ionian Sea sequence (S2) obtained from the Template Matching catalog. (a) Vertical cross-section along the SW-NE direction showing the spatial distribution of the earthquakes beneath the Ionian Sea. (b) Magnitude histogram of the relocated events, showing a predominance of low-magnitude earthquakes, with most events between about ML 1.5 and 2.3 and a minimum detected magnitude of ML 1.2.

Sequence 3: Messina Strait swarm

The third sequence correspond to a small seismic swarm that occurred in the Messina Strait between May 31 to June 1, 2022. During these two days, the real-time surveillance system detected 44 events, with local magnitudes ranging between ML 0.3 and 2.0. The subsequent BSI review increased the number of located earthquakes to 58 (approximately 30% more), without lowering minimum reported magnitude.

After relocation with the NonLinLoc program, the seismicity delineated a compact cluster confined within a small volume at depths between approximately 7-10 km (Fig. 14a). In this area, the dense distribution of FXLand stations

along the coast near Messina (Sicily) and Reggio Calabria (Calabria) provides a particularly favorable network geometry, resulting in improved detection capability and tighter constraints on hypocentral locations.

The application of the Template Matching technique to the integrated RSN+FXLand dataset led to a marked increase in detected seismicity, with the number of earthquakes rising from 44 to 107. This approach also allowed the detection of events with negative local magnitudes (Fig. 14b).

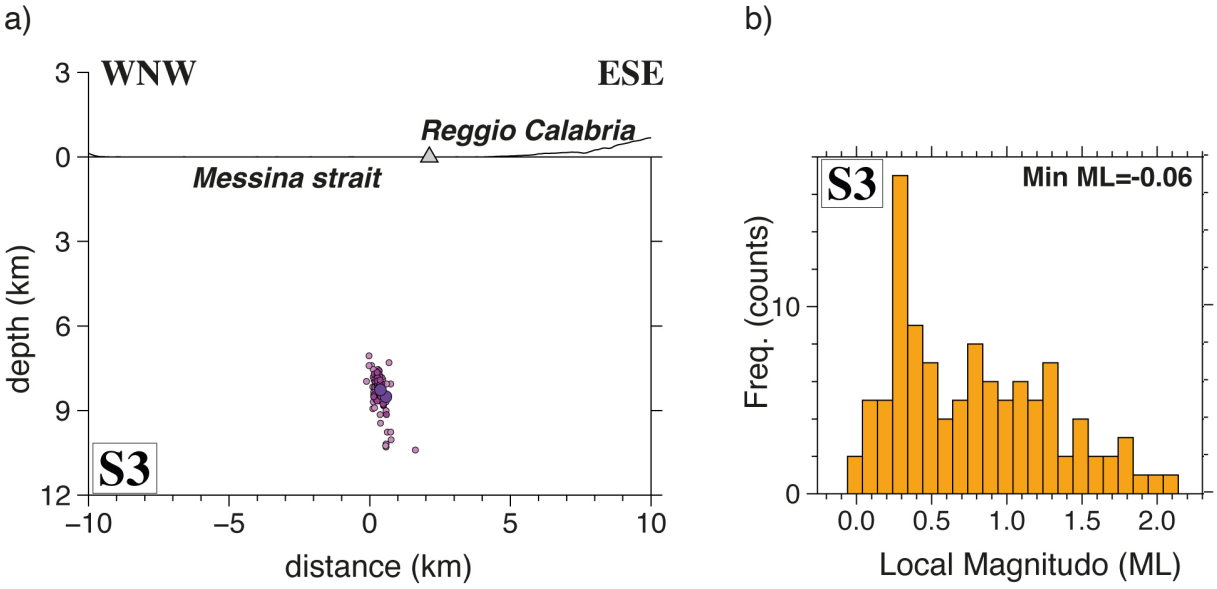

Figure 14. Relocated seismicity of the Messina Strait swarm (S3) obtained from the Template Matching catalog. (a) Vertical cross-section along the WNW-ESE direction showing the spatial and depth distribution of the earthquakes beneath the Messina Strait. (b) Magnitude histogram of the relocated events, showing a predominance of low-magnitude earthquakes, with most events below ML 1.0 and a minimum detected magnitude of ML −0.06.

A quantitative summary of the three analyzed seismic sequences is provided in Table 2, which compares, for each sequence, the number of detected earthquakes and the minimum reported magnitude obtained from routine real-time processing, the BSI review, and the Template Matching analysis. This comparison highlights the systematic increase in catalog completeness achieved through the application of the TM technique to the integrated RSN+FXLand dataset.

Table 2. Summary of the three seismic sequences analyzed in this study. For each sequence, the table reports the number of events detected by the real-time surveillance system (RT), after revision by the Italian Seismic Bulletin (BSI), and using the Template Matching (TM) technique, together with the corresponding minimum local magnitudes.

Sequence	Time interval	Sequence type	N (RT)	N (BSI)	N (TM)	MLmin (RT)	MLmin (BSI)	MLmin (TM)
S1	Dec 23, 2021 – Jan 2022	Aftershock sequence	52	80	128	1.17	1.13	0.63
S2	Feb 6 – Apr 27, 2022	Offshore sequence	30	30	30	1.2	1.2	1.2
S3	May 31 – Jun 1, 2022	Seismic swarm	44	58	107	0.3	0.3	<0

Although the analysis of the three seismic sequences provides a detailed quantitative description of the detected seismicity, the available data do not support robust geostructural interpretations of the activated fault

systems. The limited observation period, the exclusive use of land-based stations, and the offshore location of part of the seismicity constrain the resolution achievable for fault geometry and structural characterization. Moreover, a detailed seismotectonic interpretation was not the primary objective of this study, which instead focuses on evaluating the contribution of the FXLand temporary network to seismic monitoring and earthquake detection.

More stringent constraints on fault geometry and activity along the Ionian margin would require the integration of the onshore FXLand dataset with offshore observations from the FXOBS ocean-bottom seismometer network. Such an integrated analysis, which is beyond the scope of the present work, represents a natural next step for improving the characterization of offshore seismicity in this region.

5. Conclusions

The FXLand temporary seismic network was deployed along the Ionian coasts of Sicily and Calabria with the aim of enhancing seismic monitoring in a region characterized by complex seismotectonics and a significant proportion of offshore earthquake sources. The integration of 13 temporary stations into the INGV real-time surveillance system between December 2021 and June 2023 resulted in denser coastal coverage and a substantial reduction in the distance between seismic stations and offshore source areas.

A systematic assessment of data quality demonstrated that, despite elevated ambient noise levels typical of coastal and urban environments, the FXLand stations provided stable and reliable recordings suitable for both real-time surveillance and post-processing analyses. Differences in noise characteristics among stations are consistent with sensor type, installation geometry, and local site conditions, and do not indicate instrumental limitations. The open dissemination of the FXLand dataset through EIDA, together with the assignment of a DOI, ensures long-term accessibility and reuse by the scientific community.

The integration of FXLand stations into the national surveillance workflow and the Italian Seismic Bulletin significantly increased the number of available phase pickings and improved hypocentral constraints. A dedicated relocation test comparing the permanent RSN-only configuration with the combined RSN+FXLand network shows that the temporary coastal deployment contributes to reducing azimuthal gaps, shortening epicentral distances to the nearest station, and decreasing formal location uncertainties for both onshore and near-offshore earthquakes.

The application of advanced processing techniques, such as Template Matching, to the integrated RSN+FXLand dataset further enhanced earthquake detection. The analysis of three representative seismic sequences illustrates how the combined use of dense coastal station coverage and correlation-based detection methods increases catalog completeness, particularly for low-magnitude events in onshore settings, with improvements of up to a factor of approximately 2-3 relative to real-time analyses. In contrast, the offshore sequence highlights the intrinsic limitations of land-only networks for constraining submarine seismicity, even when augmented by temporary coastal deployments.

Overall, these results demonstrate that temporary onshore networks such as FXLand can effectively complement permanent seismic infrastructures by improving coastal monitoring and supporting advanced data-processing workflows. However, a comprehensive characterization of offshore seismicity along the Ionian margin requires the integration of land-based observations with marine datasets. The joint analysis of FXLand data with the FXOBS ocean-bottom seismometer network, which is beyond the scope of this study, represents a necessary next step toward reducing location uncertainties and better resolving active fault systems in the Ionian Sea.

Focus Working Group 2021 (https://progetti.ingv.it/it/focus#focus-working-group, last accessed February 2025).
INGV Osservatorio Nazionale Terremoti: Lucia Margheriti, Milena Moretti, Antonio Costanzo, Pierdomenico Del Gaudio, Sergio Falcone, Anna Gervasi, Aladino Govoni, Diana Latorre, Alfonso Mandiello, Alessandro Marchetti, Anna Nardi, Marina Pastori, Stefano Pintore, Salvatore Stramondo.
INGV Osservatorio Etneo: Salvatore Alparone, Ornella Cocina, Danilo Contrafatto, Sergio Di Prima, Graziano Larocca, Salvatore Rapisarda, Luciano Scuderi.
Laboratorio di Sismologia Università della Calabria: Mario La Rocca, Michela Ponte (PhD student), Lorenzo Festa.
Geo-Ocean UMR6538, CNRS – IFREMER – Univ. Bretage Occidentale – Univ. Bretagne Sud: Marc-Andre Gutscher, Shane Murphy, Chastity Aiken.

Data availability statement. Earthquake waveforms can be downloaded at http://eida.rm.ingv.it/, and pickings are available at https://bsi.ingv.it/it/archivio-dati.

Acknowledgements. The FOCUS project is funded by the European Research Council Advanced Grant FOCUS #786304. We extend our gratitude to the "Arma dei Carabinieri" for their availability and invaluable logistical support within the FOCUS project. We wish to thank all the personnel from the headquarters in Sicily and Calabria who hosted our instrumentation and continue to assist us, ensuring the stations operate at their best.
A special thanks goes to CoReMo and our colleagues from the ONT – Laboratorio Reti Sismiche in Rome for their technical support in assembling and configuring the stations. We are grateful to Stefano Farroni, Sandro Rao, Ulderico Piccolini, Edoardo Giandomenico, Fabio Criscuoli and Andrea Serratore for their dedication and expertise.
Finally, we sincerely thank the Editor-in-Chief, Paola Montone, the Guest Editors, Gergana Georgieva and Irene Molinari, and the anonymous reviewer and Petr Kolínský for their careful evaluation of the manuscript and for their constructive comments and suggestions, which significantly contributed to improving the clarity and quality of this work.

References

Basili, R., G. Valensise, P. Vannoli, P. Burrato et al. (2008). The Database of Individual Seismogenic Sources (DISS), version 3: summarizing 20 years of research on Italy's earthquake geology, Tectonophysics, doi:10.1016/j.tecto.2007.11.031.

Bruni, R., L. Lenti, C. Martino, A. Piscitelli et al. (2022). A temporary network for monitoring seismicity in the Mugello basin (Northern Apennines, Italy), INGV Technical Report.

BSI Working Group (2015). Bollettino Sismico Italiano, BSI, Istituto Nazionale di Geofisica e Vulcanologia, INGV, doi:10.13127/bsi.

Cogliano, R., M. Pischiutta, S. Hailemikael, G. Franceschina et al. (2021). Indicators for the quality assessment of temporary seismic network stations installed on soft-soil sites, Bull. Earthq. Eng., 19, 3, 1361-1386, doi:10.1007/s10518-021-01136-7.

D'Agostino N., A. Avallone, D. Cheloni, E. D'Anastasio et al. (2008). Active tectonics of the Adriatic region from GPS and earthquake slip vectors, J. Geophys. Res., 113, B12413, doi:10.1029/2008JB005860.

Danecek, P., S. Pintore, S. Mazza, A. Mandiello et al. (2021). The Italian Node of the European Integrated Data Archive, Seismol. Res. Lett., 92, 3, 1726-1737, doi:10.1785/0220200409.

Dellong, D., F. Klingelhoefer, H. Kopp, D. Graindorge et al. (2018). Crustal structure of the Ionian basin and eastern Sicily margin: Results from a wide-angle seismic survey, J. Geophys. Res., Solid Earth, 123, 2090-2114, doi:10.1002/2017JB015312.

Devoti, R., F. Riguzzi, M. Cuffaro and C. Doglioni (2008). New GPS constraints on the kinematics of the Apennines subduction, Earth Planet. Sci. Lett., 273, 163-174, doi:10.1016/j.epsl.2008.06.031.

DISS Working Group (2025, March 28). Database of Individual Seismogenic Sources (DISS), version 3.3.1: A compilation of potential sources for earthquakes larger than M 5.5 in Italy and surrounding areas, Istituto Nazionale di Geofisica e Vulcanologia, INGV, doi:10.13127/diss3.3.1.

Fiorentino, A., M. Agate, L. Battaglini, M. Busetti et al. (2025). Structural map of seas surrounding Italy, ISPRA, doi:10.15161/oar.it/7m0x6-rbn31.

Gambino, S., G. Barreca, V. Bruno, G. De Guidi et al. (2022). Transtension at the Northern Termination of the Alfeo-Etna Fault System (Western Ionian Sea, Italy): Seismotectonic Implications and Relation with Mt. Etna Volcanism, Geosciences, 12,128, doi:10.3390/geosciences12030128.

Gibbons, S. J. and F. Ringdal (2006). The detection of low magnitude seismic events using array-based waveform correlation, Geophys. J. Int., 165, 149-166, doi:10.1111/j.1365-246X.2006.02865.x.

Giuffrida, S., F. Brighenti, F. Cannavò, F. Carnemolla et al. (2023). Multidisciplinary analysis of 3D seismotectonic modelling: A case study of Serre and Cittanova faults in the southern Calabrian Arc (Italy), Front. Earth Sci., 11, 1240051, doi:10.3389/feart.2023.1240051.

Guidoboni, E., G. Ferrari, D. Mariotti, A. Comastri et al. (2018). CFTI5Med, Catalogo dei Forti Terremoti in Italia (461 a.C.-1997) e nell'area Mediterranea (760 a.C.-1500), Istituto Nazionale di Geofisica e Vulcanologia, INGV, doi:10.6092/ingv.it-cfti5.

Guidoboni, E., G. Ferrari, G. Tarabusi, G. Sgattoni et al. (2019). CFTI5Med, the new release of the catalogue of strong earthquakes in Italy and in the Mediterranean area, Scientific Data, 6, 80, doi:10.1038/s41597-019-0091-9.

Gutscher, M. A., H. Kopp, S. Krastel, G. Bohrmann et al. (2017). Active tectonics of the Calabrian subduction revealed by new multi-beam bathymetric data and high-resolution seismic profiles in the Ionian Sea (Central Mediterranean), Earth Planet. Sci. Lett., 461, 61-72, doi:10.1016/j.epsl.2016.12.020.

Husen, S. and R. B. Smith (2004). Probabilistic Earthquake Relocation in Three-Dimensional Velocity Models for the Yellowstone National Park Region, Wyoming, Bulletin of the Seismological Society of America, Vol 94, No. 3, pp. 880-896, June 2004, doi:10.1785/0120030170.

Istituto Nazionale di Geofisica e Vulcanologia (2005). Rete Sismica Nazionale, RSN, Data set, Istituto Nazionale di Geofisica e Vulcanologia, INGV, doi:10.13127/SD/X0FXNH7QFY.

INGV Data Management Office (2020). INGV Open Data Registry, the metadata catalogue of the Istituto Nazionale di Geofisica e Vulcanologia, Data set, Istituto Nazionale di Geofisica e Vulcanologia, INGV, doi:10.13127/data-registry.

Kissling, E., W. L. Ellsworth, D. Eberhart-Phillips and U. Kradolfer (1994). Initial reference models in local earthquake tomography, J. Geophys. Res., Solid Earth, 99, B10, 19635-19646, doi:10.1029/93JB03138.

Kolínský, P., T. Meier, M. R. Agius, A. Bijedić et al. (2025). AdriaArray – a Passive Seismic Experiment to Study Structure, Geodynamics and Geohazards of the Adriatic Plate, Ann. Geophys., 68, 5, DM555, doi:10.4401/ag-9284.

Latorre, D. and R. Di Stefano (2024). PRECISE: PRobabilistic Earthquake location Catalog of the Italian SEismicity in 3D tomographic models and 1D regional velocity models, in Giornata ONT 2023 Proceedings Volume Stramondo S., Moretti M., Bignami C., Nardi A. et al. (Eds.), Rome 14th November 2023, Misc. INGV, 79, 184-185, doi:10.13127/misc/79.

Lomax, A., J. Virieux, P. Volant and C. Berge-Thierry (2000). Probabilistic earthquake location in 3D and layered models, in Advances in Seismic Event Location. Modern Approaches in Geophysics Thurber C. H., Rabinowitz N. (Eds.), 18. Springer, Dordrecht, The Netherlands, 101-134, doi:10.1007/978-94-015-9536-0_5.

Lomax, A., A. Michelini and A. Curtis (2014). Earthquake location, direct, global-search methods, in Encyclopedia of Complexity and System Science Meyers R. A. (Ed.), Second Ed. Springer, New York, 1-33, doi:10.1007/978-3-642-27737-5_150-2.

Maesano, F. E., M. M. Tiberti and R. Basili (2018). The Calabrian Arc: three-dimensional modelling of the subduction interface, Sci. Reports, 7, 8887, doi:10.1038/s41598-017-09074-8.

Maesano, F. E., M. M. Tiberti and R. Basili (2020). Deformation and Fault Propagation at the Lateral Termination of a Subduction Zone: The Alfeo Fault System in the Calabrian Arc, Southern Italy, Front. Earth Sci, 8,107, doi:10.3389/feart.2020.00107.

Margheriti, L., M. Moretti, C. Aiken, S. C. Alparone et al. (2024). La rete sismica temporanea FXLand: contribuito al Progetto Fiber Optic Cable Use For Seafloor Studies Of Earthquake – FOCUS, Rapp. Tec. INGV, 479, 1-26, doi:10.13127/rpt/479.

McNamara, D. E. and R. P. Buland (2004). Ambient noise levels in the continental United States, Bull. Seismol. Soc. Am., 94, 4, 1517-1527, doi:10.1785/012003001.

MedNet Project Partner Institutions (1990). Mediterranean Very Broadband Seismographic Network, MedNet, Data set, Istituto Nazionale di Geofisica e Vulcanologia, INGV, doi:10.13127/SD/FBBBTDTD6Q.

Meletti, C., V. Montaldo, M. Stucchi and F. Martinelli (2006). Database della pericolosità sismica MPS04, Istituto Nazionale di Geofisica e Vulcanologia, INGV, doi:10.13127/SH/MPS04/DB.

Moretti, M., A. Govoni, G. Colasanti, M. Silvestri et al. (2010). La Rete Sismica Mobile del Centro Nazionale Terremoti, Rapp. Tec. INGV, 137, 1-66, http://hdl.handle.net/2122/5982.

Moretti, M., L. Margheriti, S. C. Alparone, A. Costanzo et al. (2021). Seismic Data acquired by FocusX temporary land-network (FXland), Southern Italy, Data set, Istituto Nazionale di Geofisica e Vulcanologia, INGV, doi:10.13127/sd/o5qwm6wjcd.

Moretti, M., L. Margheriti, E. D'Alema and D. Piccinini (2023). SISMIKO: INGV operational task force for rapid deployment of seismic network during earthquake emergencies, Front. Earth Sci., 11, 1146579, doi:10.3389/feart.2023.1146579.

Pastori, M., D. Latorre, L. Margheriti and L. Scognamiglio (2020). Inquadramento sismotettonico delle macroaree appartenenti al territorio italiano, Zenodo, doi:10.5281/zenodo.10687348.

Peterson, J. (1993). Observations and modeling of seismic background noise, U. S. Geological Survey Open File Report, 93-322, doi:10.3133/ofr93322.

Polonia, A., L. Gasperini and L. Torelli (2011). The Calabrian Arc subduction complex in the Ionian Sea: Regional architecture, active deformation, and seismic hazard, Tectonics, doi:10.1029/2010TC002821.

Polonia, A., L. Torelli, A. Artoni, M. Carlini et al. (2016). The Ionian and Alfeo-Etna fault zones: New segments of an evolving plate boundary in the central Mediterranean Sea?, Tectonophysics, 675, 69-90, doi:10.1016/j.tecto.2016.03.016.

Puglisi, G., R. Basili, A. G. Chiodetti, A. Cianchi et al. (2018). La Politica dei Dati dell'INGV/The INGV Data Policy, Istituto Nazionale di Geofisica e Vulcanologia, INGV, https://hdl.handle.net/2122/14886.

Rossi, S. and R. Sartori (1981). A seismic reflection study of the External Calabrian Arc in the northern Ionian Sea (eastern Mediterranean), Mar. Geophys. Res., 4, 403-426, doi:10.1007/BF00286036.

Serpelloni, E., G. Vannucci, S. Pondrelli, A. Argnani et al. (2007). Kinematics of the Western Africa-Eurasia plate boundary from focal mechanisms and GPS data, Geophys. J. Int., 169, 3, 1180-1200, doi:10.1111/j.1365-246X.2007.03367.x.

Serpelloni, E., R. Bürgmann, M. Anzidei, P. Baldi et al. (2010). Strain accumulation across the Messina Straits and kinematics of Sicily and Calabria from GPS data and dislocation modeling, Earth Planet. Sci. Lett., 298, 3-4, 347-360, doi:10.1016/j.epsl.2010.08.005.

Shelly, D. R., G. C. Beroza and S. Ide (2007). Non-volcanic tremor and low-frequency earthquake swarms, Nature, 446, 305-307, doi:10.1038/nature05666.

Sgroi, T., A. Polonia, G. Barberi, A. Billi et al. (2021). New seismological data from the Calabrian arc reveal arc-orthogonal extension across the subduction zone, Sci. Rep., 11, 473, doi:10.1038/s41598-020-79719-8.

Sgroi, T., G. Barberi, L. Gasperini, R. Govers et al. (2025). Structural development and seismogenesis in the Messina Straits revealed by stress/strain pattern above the edge of the Calabrian slab (Central Mediterranean), Tectonophysics, 915, 230920, doi:10.1016/j.tecto.2025.230920.

Stucchi, M., C. Meletti, V. Montaldo, H. Crowley et al. (2011). Seismic Hazard Assessment (2003-2009) for the Italian Building Code, Bull. Seismol. Soc. Am., 101, 4, 1885-1911, doi:10.1785/0120100130.

Università della Calabria, Italy. (1981). Rete Sismica Unical, Data set, International Federation of Digital Seismograph Networks, doi:10.7914/SN/IY.

Vassallo, M., G. Festa, A. Bobbio (2012). Seismic Ambient Noise Analysis in Southern Italy, Bulletin of the Seismological Society of America, 102, 574-586, doi:10.1785/0120110018.

***CORRESPONDING AUTHOR: Marina PASTORI**,
Istituto Nazionale di Geo isica e Vulcanologia, Osservatorio Nazionale Terremoti, Rome, Italy
e-mail: marina.pastori@ingv.it